# COHERENCE PROPERTIES OF THE RADIATION FROM FLASH

E.A. Schneidmiller, M.V. Yurkov, DESY, Hamburg, Germany

## Abstract

Several user groups at FLASH use higher odd harmonics (3rd and 5th) of the radiation in experiments. Some applications require knowledge of coherence properties of the radiation at he fundamental and higher harmonics. In this paper we present the results of the studies of coherence properties of the radiation from FLASH operating at radiation wavelength of 8.x nm at the fundamental harmonic, and higher odd harmonics (2.x nm and 1.x nm). We found that present configuration of FLASH free electron laser is not optimal for providing ultimate quality of the output radiation. Our analysis shows that the physical origin of the problem is mode degeneration. The way for improving quality of the radiation is proposed.

## INTRODUCTION

After an energy upgrade the soft X-ray FEL FLASH at DESY covers a spectral range between approximately 45 nm and 4.2 nm wavelength [1, 2]. With the present undulator (period 2.73 cm, peak field 0.486 T) the minimum wavelength of 4.2 nm is determined by the maximum electron beam energy of approximately 1.25 GeV. There exists clear tendency for users at FLASH to extend available wavelength range to shorter wavelengths. Here we first remember about the so-called water window, i.e. the range between the K-Absorption edges of carbon and oxygen at 4.38nm and 2.34 nm, respectively. Currently minimum wavelength of FLASH is just below the carbon edge. Other range of interest refers to the edges of magnetic elements which spans below water window. In principle, higher odd harmonics of SASE radiation can be used to get radiation. Pioneer experiment for studying magnetic materials using FEL radiation has been performed at FLASH at 1.6 nm wavelength, the 5th harmonic of the fundamental at 8 nm [3]. Many user's experiments rely on coherent properties of the radiation, both temporal and spatial. This concern relates not only to the fundamental harmonic, but to the higher odd harmonics as well.

Previous studies have shown that with given parameters of the electron beam, coherence properties of the radiation strongly evolve during amplification process. At the initial stage of amplification coherence properties are poor, and radiation consists of large number of transverse and longitudinal [4]:

$$\tilde{E} = \int \mathrm{d}\omega \exp[i\omega(z/c - t)] \qquad (1)$$
$$\times \sum_{n,k} A_{nk}(\omega, z)\Phi_{nk}(r, \omega)\exp[\Lambda_{nk}(\omega)z + in\phi]$$

described by the eigenvalue $\Lambda_{nk}(\omega)$ and the field distribution eigenfunction $\Phi_{nk}(r, \omega)$. Here $\omega = 2\pi c/\lambda$ is the frequency of the electromagnetic wave. The fundamental mode (having maximum real part of the eigenvalue) dominates more and more over higher modes when undulator length progresses. Total undulator length to saturation is in the range from about nine (hard x-ray SASE FELs) to eleven (visible range SASE FELs) field gain lengths [5, 6, 9]. Situation with transverse coherence is favorable when relative separation of increments between fundamental and higher modes is more than 20%. In this case degree of transverse coherence asymptotically approaches to unity in the amplification process, and can reach values above 90% in the end of the high gain linear regime [7, 8]. Further development of amplification process in the nonlinear stage leads to visible degradation of the spatial and temporal coherence [5, 6, 9]. Separation of the increments of the beam radiation modes strongly depends on the value of diffraction parameter, and is more pronouncing for stronger focused electron beams [10]. Increase of the energy spread and emittance also leads to better separation of the increments of the beam radiation modes.

In the present experimental situation many parameters of the electron beam at FLASH depend on practical tuning of the machine. Analysis of measurements and numerical simulations shows that depending on tuning of the machine emittance may change from about 1 to about 1.5 mm-mrad. Tuning at small charges may allow to reach smaller values of the emittance down to 0.5 mm-mrad. Peak current may change in the range from 1 kA to 2 kA depending on the tuning of the beam formation system. One (more or less) fixed parameter is average focusing beta function in the undulator which has average value about 10 meters. In this paper we perform thorough analysis of described parameter space with special attention to the coherence properties of the radiation not only for the fundamental frequency, but also for the 3rd and the 5th harmonic. Our conclusion is that spatial coherence of the radiation at FLASH suffers significantly from not sufficient suppression of the higher radiation modes. This happens due to the large value of the diffraction parameter. Our analysis shows that operation with stronger beam focusing, lower emittances and lower peak current will allow to operate FLASH with ultimate quality of the radiation in terms of the degree of transverse coherence exceeding 90%.

For illustration we have chosen specific wavelength of 8 nm. The main reason for this is that this wavelength has been used by several user groups (see, e.g. [3, 12, 13]). Thus, results, presented here, can be used directly for analysis of obtained results and planning future measurements.

## GENERAL DEFINITIONS

The first-order time correlation function $g_1(t, t')$ and transverse correlation function $\gamma_1(\vec{r}_\perp, \vec{r'}_\perp, z, t)$ are defined as

$$g_1(\vec{r}, t - t') = \frac{\langle \tilde{E}(\vec{r}, t)\tilde{E}^*(\vec{r}, t')\rangle}{\left[\langle| \tilde{E}(\vec{r}, t) |^2\rangle\langle| \tilde{E}(\vec{r}, t') |^2\rangle\right]^{1/2}},$$

$$\gamma_1(\vec{r}_\perp, \vec{r'}_\perp, z, t) = \frac{\langle \tilde{E}(\vec{r}_\perp, z, t)\tilde{E}^*(\vec{r'}_\perp, z, t)\rangle}{\left[\langle|\tilde{E}(\vec{r}_\perp, z, t)|^2\rangle\langle|\tilde{E}(\vec{r'}_\perp, z, t)|^2\rangle\right]^{1/2}},$$

where $\tilde{E}$ is the slowly varying amplitude of the amplified wave. For a stationary random process the coherence time and the degree of transverse are defined as [5]:

$$\zeta = \frac{\int |\gamma_1(\vec{r}_\perp, \vec{r'}_\perp)|^2 I(\vec{r}_\perp)I(\vec{r'}_\perp)\, \mathrm{d}\, \vec{r}_\perp\, \mathrm{d}\, \vec{r'}_\perp}{[\int I(\vec{r}_\perp)\, \mathrm{d}\, \vec{r}_\perp]^2},$$

$$\tau_\mathrm{c} = \int_{-\infty}^{\infty} |g_1(\tau)|^2\, \mathrm{d}\, \tau, \qquad (2)$$

where $I(\vec{r}_\perp) = \langle|\tilde{E}(\vec{r}_\perp)|^2\rangle$. The first order time correlation function, $g_1(t, t')$, is calculated in accordance with the definition:

Brilliance of the radiation is proportinal to the product of the radiation power, coherence time, and degree of transverse coherence. If one traces evolution of the brilliance of the radiation along the undulator length there is always the point, which we define as the saturation point, where the brilliance reaches maximum value [5]. We illustrate general definitions in Figure 1 with specific numerical example for FLASH operating at the wavelength of 8 nm, peak current 1.5 kA, and rms normalized emittance 1 mm-mrad. Radiation power continues to grow after saturation point. However, we obtain significant degradation of the spatial and temporal coherence, such that brilliance of the radiation falls down.

## SIMULATION PROCEDURE

Simulations have been performed with three-dimensional, time-dependent FEL simulation code [14]. Simulations of the statistical properties have been performed for the case of a long bunch with uniform axial profile of the beam current. Simulations cover the range of practical interest for emittances from 0.5 mm-mrad to 1.5 mm-mrad, and the range of peak currents from 1 to 2 kA. Radiation wavelength of 8 nm is chosen for detailed analysis.

## RADIATION POWER

We present in Figure 2 evolution along the undulator of the radiation power in the fundamental harmonic. Higher values of the peak current and smaller emittances would allow to reach higher radiation powers. When amplification process enters nonlinear stage, the process of nonlinear harmonic generation takes place [15–24]. Figures 3 and
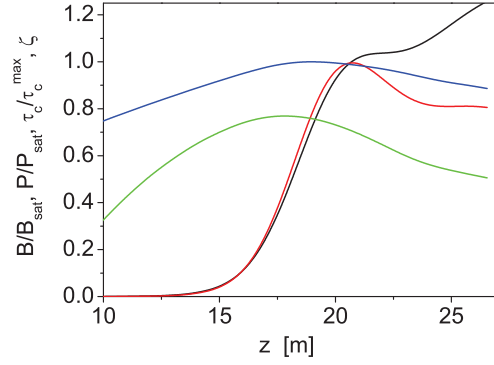


Figure 1: Evolution of the radiation power (black curve), coherence time (blue curve), degree of transverse coherence (green curve), and brilliance (red curve) along the undulator. Brilliance and radiation power are normalized to saturation values. Coherence time is normalized to maximum value of 5.5 fs. Peak current is 1.5 kA, normalized rms emittance is $\epsilon_n = 1$ mm-mrad.
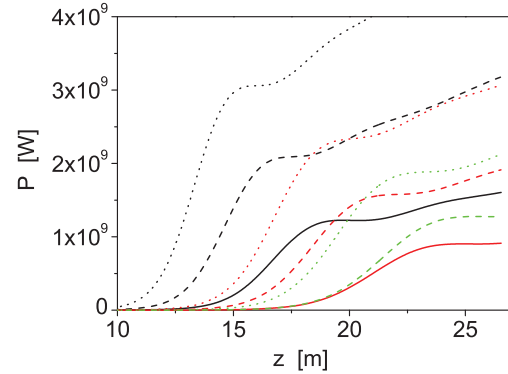


Figure 2: Evolution of the radiation power along undulator. Color codes (black, red and green) refer to different emittance $\epsilon_n = 0.5$, 1, and 1.5 mm-mrad. Line styles (solid, dash, and dot) refer to different values of peak current 1 kA, 1.5 kA, and 2 kA.

4 show relevant contribution to the total power of the 3rd and the 5th harmonic. Saturation point and total undulator length (27 m) are chosen as reference points. General observation is that relative contribution of the higher harmonic is higher for smaller values of the emittance. With the value of the normalized emittance of 1 mm-mrad, partial contributions for the 3rd and the 5th harmonic are in the range of $0.7 - 1 \times 10-2$ and $2 - 2.5 \times 10-4$, respectively. Note that this result is pretty much close to that described by universal scaling with an appropriate correction for longitudinal velocity spread derived in [24]:

$$\frac{\langle W_3 \rangle}{\langle W_1 \rangle}\big|_\mathrm{sat} = 0.094 \times \frac{K_3^2}{K_1^2},$$

$$\frac{\langle W_5 \rangle}{\langle W_1 \rangle}\big|_\mathrm{sat} = 0.03 \times \frac{K_5^2}{K_1^2}. \qquad (3)$$
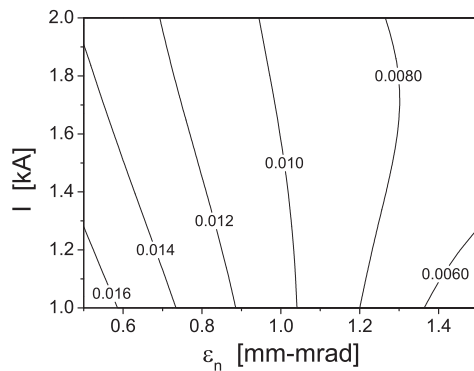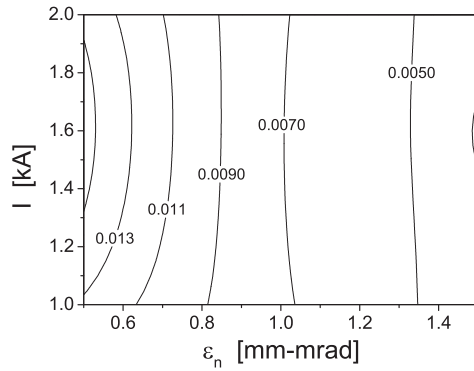
Figure 3: Partial contribution of the 3rd harmonic to the total power versus peak beam current and emittance. Top and bottom plot refer to the saturation point and the undulator end, respectively.
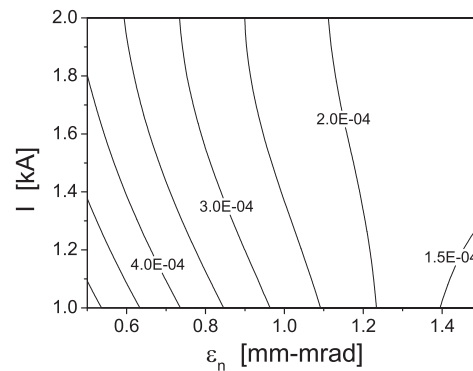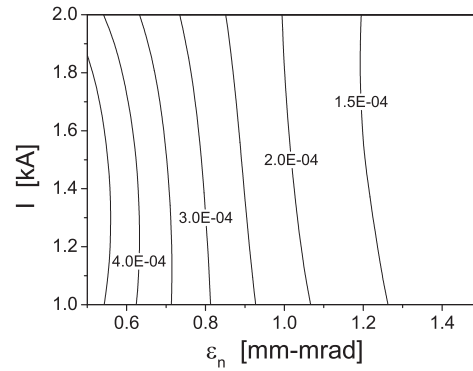


Figure 4: Partial contribution of the 5th harmonic to the total power versus peak beam current and emittance. Top and bottom plot refer to the saturation point and the undulator end, respectively.

Here $K_h = K(-1)^{(h-1)/2}[J_{(h-1)/2}(Q) - J_{(h+1)/2}(Q)]$, $Q = K^2/[2(1 + K^2)]$, $K$ is rms undulator parameter, and $h$ is an odd integer - harmonic number.

## TEMPORAL COHERENCE

In the framework of the one-dimensional model the coherence time in the saturation point is described in terms of FEL parameter $\rho$ [25] and number of cooperating electrons $N_c = I/(e\rho\omega)$ [10]:

$$\tau_c \simeq \frac{1}{\rho\omega}\sqrt{\frac{\pi \ln N_c}{18}}.$$

The coherence time of higher harmonics in the saturation point and in the post-saturation amplification stage scales inversely proportional to the harmonic number, while relative spectrum bandwidth remains constant with the harmonic number.

Blue curve in Fig. 1 shows evolution of the coherence time which is typical for all SASE FELs. In the high gain linear regime it falls down as a square root of undulator length. It reaches maximum value just before saturation point, and then it drops down. Figures 5 show coherence time for the whole parameter range for the fundamental harmonic. Coherence time for the higher harmonic can be derived using scaling described above.

## SPATIAL COHERENCE

Figure 6 presents an overview of the degree of transverse coherence in the complete parameter space. Brief view on these plots tells us that the degree of transverse coherence for the 1st harmonic is visibly lower than ultimate value above 0.9. The reason for reduction of the spatial coherence is in the feature which is called mode degeneration. This physical phenomena takes place at large values of the diffraction parameter [10]. Figure8 shows contribution of higher azimuthal modes to the total power for specific example of emittance 1 mm-mrad and peak current 1.5 kA . Contribution of the first azimuthal modes falls down in the high gain linear regime, but to the value of 12% only, and then starts to grow in the nonlinear regime, and reaches the value of 16% at the undulator end. This results in the degree of transverse coherence of only 50%.

Higher harmonics are derived from the nonlinear process governed by the fundamental harmonic. As a result, coherence properties of the harmonics follow the same tendencies as the fundamental, but with visibly lower degree of transverse coherence [9].

## INTENSITY DISTRIBUTIONS

The feature of poor transverse coherence is reflected in the field distributions. Left plot in Fig. 9 shows typical in-
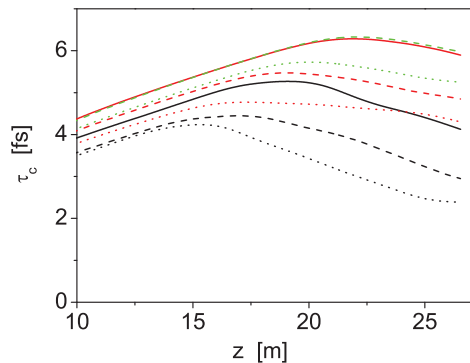
Figure 5: Evolution along undulator of the coherence time of the radiation at the fundamental frequency. Radiation wavelength is 8 nm. Color codes (black, red and green) refer to different emittance $\epsilon_n = 0.5$, 1, and 1.5 mm-mrad. Line styles (solid, dash, and dot) refer to different values of peak current 1 kA, 1.5 kA, and 2 kA.

tensity distribution over single slice. We see that transverse intensity pattern has rather complicated shape due to interference of fields of statistically independent modes. Shape of the intensity distributions changes on a scale of coherence length. Averaging of slice distributions along long pulse results in a smooth axisymmetric distribution from which we can extract averaged intensity distributions (see Fig. 10). Intensity distributions for the fundamental harmonic are always wider than those for higher frequency harmonic.

Now we pay special attention of the reader to one fundamental problem which relates to the poor transverse coherence. Right plot in Fig. 9 shows intensity profile of a typical single photon pulse with 50 fs duration (or, about ten coherence lengths). Cross at this plot shows the center of gravity of the radiation intensity averaged over many pulses. We see that the center of gravity of single shot is visibly shifted off axis. Spot shape of a short radiation pulse changes from pulse to pulse. Position of the pulse also jumps from shot to shot which is frequently referred as bad pointing stability. However, in our case bad pointing stability has fundamental origin in poor transverse coherence, but not in unstable operation of the accelerator systems. It is our practical experience from FLASH that an effect of poor pointing stability becomes more pronouncing for shorter pulses.

## DISCUSSION

Simulations presented in this paper trace nearly complete range of parameter space of FLASH in terms of emittance and peak current. Detailed illustration is presented for specific wavelength of 8 nm. We found that the radiation has relatively poor transverse coherence. This happens because FLASH FEL operates in the parameter space when different radiation modes have close values of the gain. In other words, and effect of mode degeneration takes

place. Figure of merit here is the diffraction parameter presenting the ratio of the electron beam size to the diffraction expansion of the radiation on a scale of the field gain length [10]. Power of the effect becomes stronger at the increase of the electron beam size. In the parameter space of FLASH diffraction parameter is in the range between 10 and 20. According to earlier studies ( [10], Chapter 5), gain of the first azimuthal mode $TEM_{01}$ approaches to the gain of the ground $TEM_{00}$ mode. Quality of the electron beam is high (small longitudinal velocity spread due to emittance and energy spread) which is not sufficient to suppress the gain of the higher modes. The plot in Fig. 11 traces the ratio of the field gain of the first azimuthal mode $TEM_{01}$ to the gain of the ground FEL mode $TEM_{00}$ versus radiation wavelength. We see that situation with mode selection is unfavorable in the whole wavelength range of FLASH. Ratio is nearly constant which means that detailed results for 8 nm wavelength can be referred to the whole parameter space.

Reasonable question arises: what can we do for improving situation with transverse coherence at FLASH? A straightforward way to avoid mode degeneration effect is to reduce electron beam size. Currently FLASH operates with average focusing function of 10 meters. Hardware allows to organize stronger focusing with average focusing beta function down to 5 meters. Figure 12 shows that this action would allow more strong separation of the modes. Another hint would be operation at smaller peak currents and lower emittances, say 1 kA and 0.5 mm-mrad. Our simulations show that with both actions we can easily reach ultimate degree of the transverse coherence of the radiation exceeding 90%.

We can also use another mechanism for suppression of the effect of the mode degeneration. In fact, increase of the energy spread in the electron beam leads to stronger suppression of higher beam radiation modes [10]. Increase of the energy spread can be done with laser heater [11]. Features of this effect are demonstrated with Fig. 13. Increase of the rms energy spread to the value of 0.8 MeV in terms of mode separation is equivalent to the reduction of the beta function from 10 to 5 meters. However, the price for this improvement is significant reduction of the gain of the fundamental mode and of the FEL power, while reduction of the beta function improves these important FEL parameters.

In view of results obtained we conclude that FLASH (and FLASH2) should be operated with stronger focusing of the electron beam to provide good spatial coherence of the radiation. Future developments (like design of a new undulator for FLASH) should also take into account this problem and provide relevant technical solutions for keeping small size of the electron beam in the undulator.
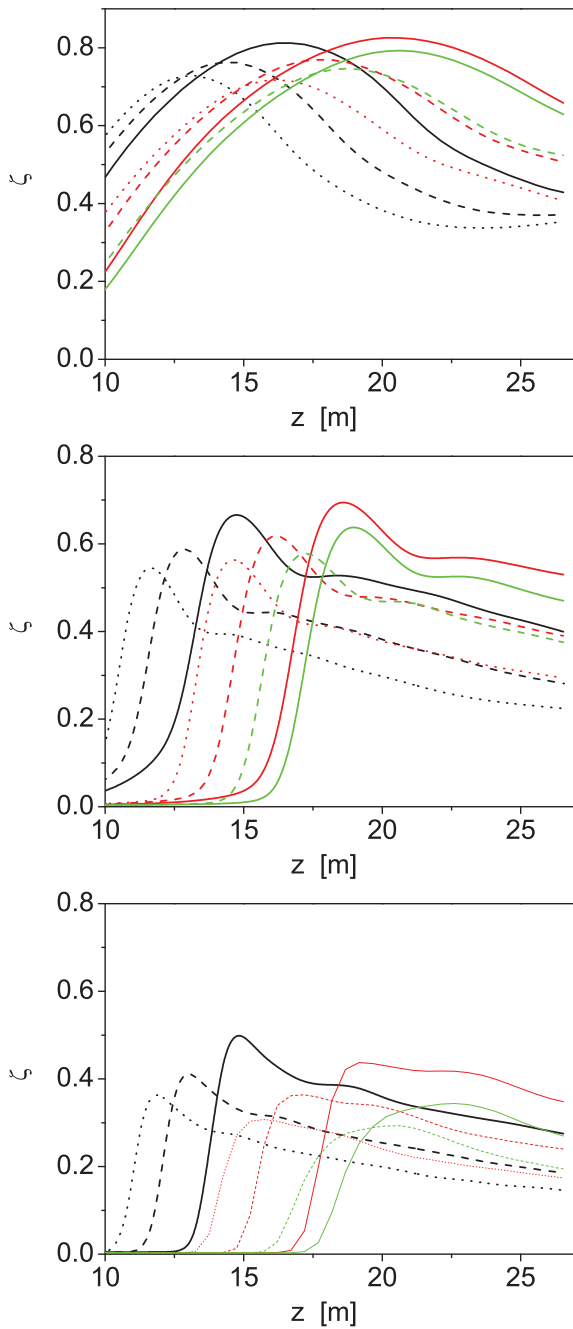
Figure 6: Evolution along undulator of the degree of transverse coherence of the radiation. Top, middle, and bottom plots correspond to the fundamental frequency (8 nm), 3rd harmonic (2.66 nm), and 5th harmonic (1.6 nm). Color codes (black, red and green) refer to different emittance $\epsilon_n = 0.5$, 1, and 1.5 mm-mrad. Line styles (solid, dash, and dot) refer to different values of peak current 1 kA, 1.5 kA, and 2 kA.
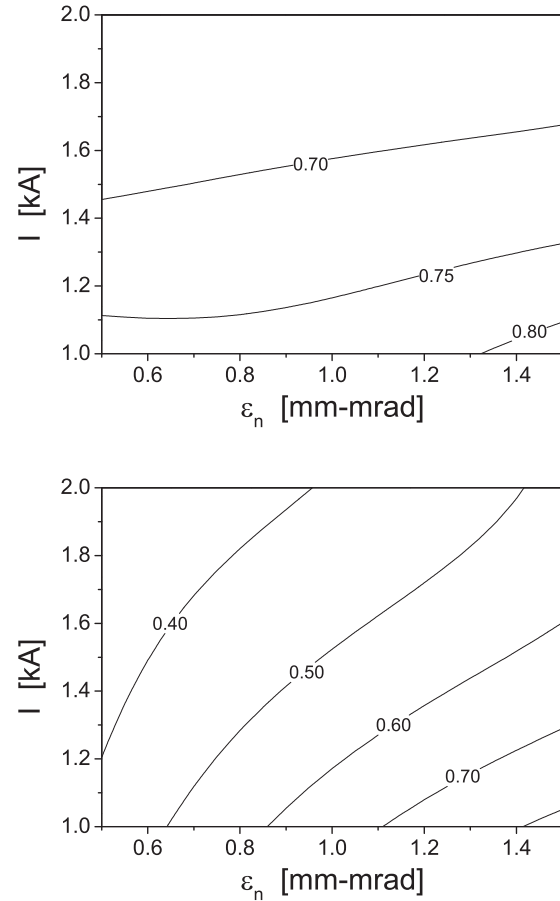


Figure 7: Degree of transverse coherence of the radiation for fundamental harmonic versus peak beam current and emittance. Top and bottom plot refer to the saturation point and the undulator end, respectively.
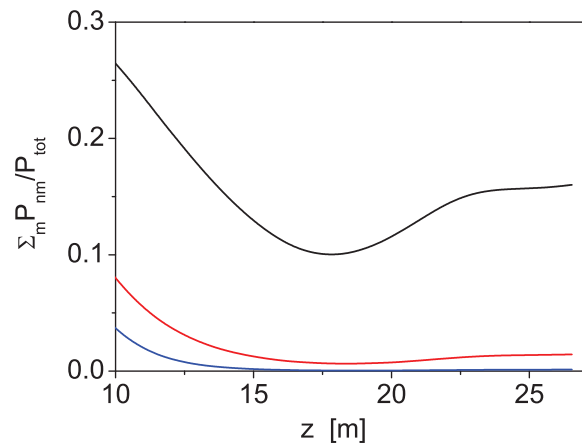


Figure 8: Partial contribution of the higher azimuthal modes of the fundamental harmonic to the total radiation power. Peak current is 1.5 kA, rms normalized emittance is 1 mm-mrad. Black, red, and green curves refer to the modes with $n = \pm1$, $n = \pm2$, and $n = \pm3$, respectively.
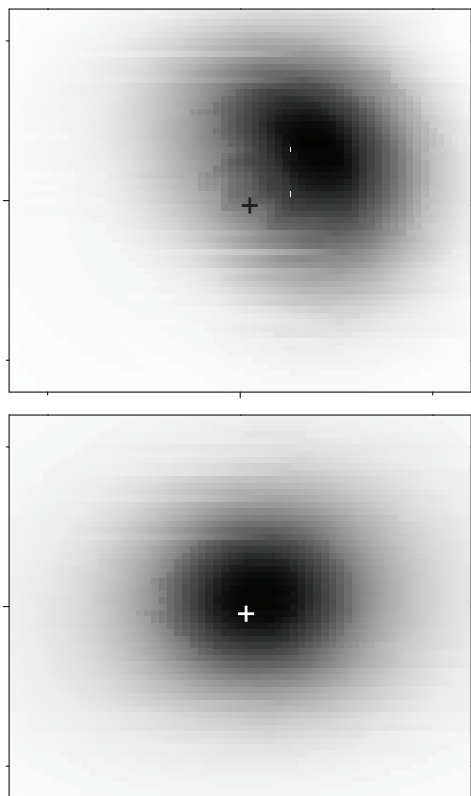
Figure 9: Profiles of the radiation at the 1st harmonic at the exit of undulator. Peak current is 1.5 kA, rms normalized emittance is 1 mm-mrad. Top: typical intensity distribution over single slice. Bottom: typical single shot with average energy in the radiation pulse of 100 microjoules (radiation pulse length 50 fs). Crosses on the plots show center of gravity of radiation intensity averaged over many pulses.
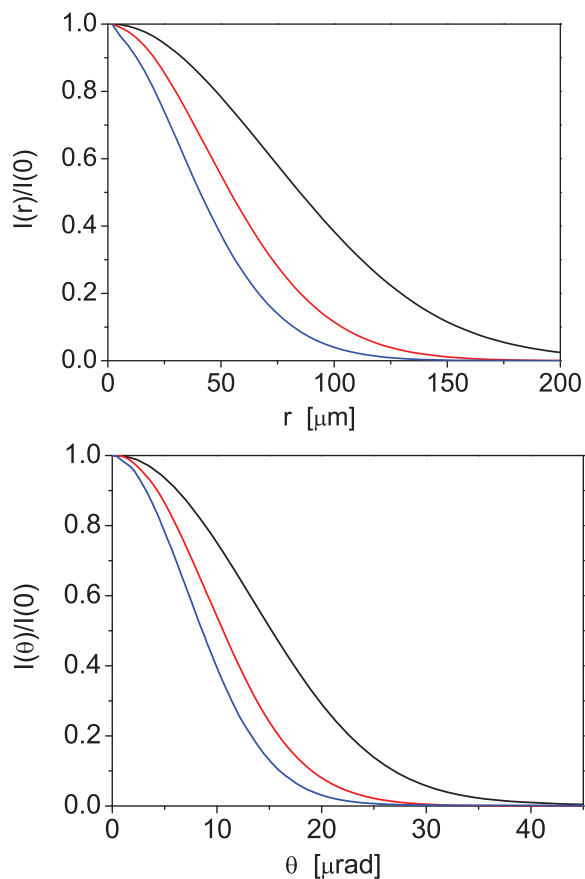
Figure 10: Intensity distribution of the radiation in the saturation point in the near zone (top plot) and far zone (bottom plot). Peak current is 1.5 kA, rms normalized emittance is 1 mm-mrad. Black, red, and green curves refer to the 1st, 3rd, and the 5th harmonic, respectively.
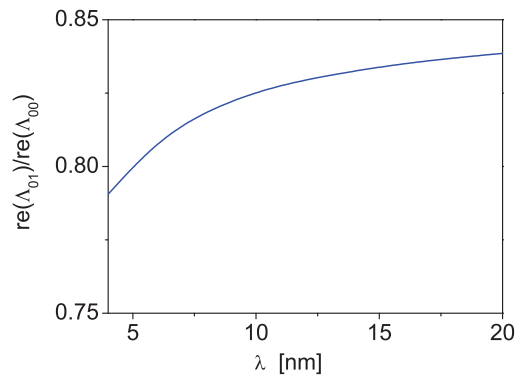
Figure 11: Ratio of the field gain of the first azimuthal mode $TEM_{01}$ to the gain of the ground FEL mode $TEM_{00}$ versus radiation wavelength. Peak current is 1.5 kA, rms normalized emittance is 1 mm-mrad. Focusing beta function is 10 m.
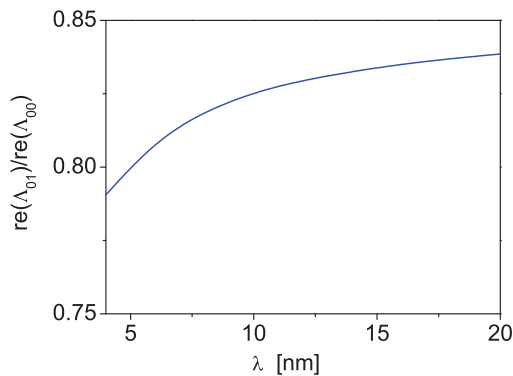


Figure 12: Ratio of the field gain of the first azimuthal mode $TEM_{01}$ to the gain of the ground FEL mode $TEM_{00}$ versus focusing beta function. Radiation wavelength is 8 nm, peak current is 1.5 kA, rms normalized emittance is 1 mm-mrad.
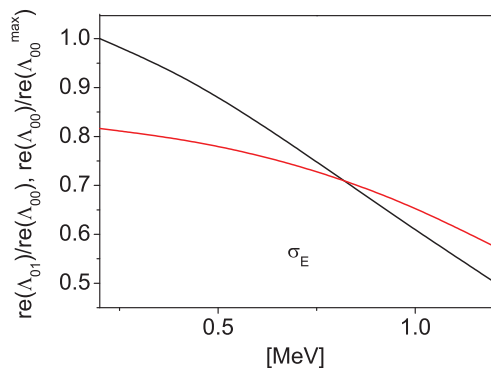


Figure 13: Ratio of the field gain of the first azimuthal mode $TEM_{01}$ to the gain of the ground FEL mode $TEM_{00}$ versus rms energy spread in the electron beam (blue curve). Black dashed curve shows relative reduction of the gain of the fundamental $TEM_{00}$ mode. Radiation wavelength is 8 nm, peak current is 1.5 kA, rms normalized emittance is 1 mm-mrad. Focusing beta function is 10 m.

# REFERENCES

[1] S. Schreiber et al., Proc. of FEL 2012 Conference, http://accelconf.web.cern.ch/AccelConf/FEL2012/papers/mopd01.pdf

[2] M. Vogt et al., Proc. IPAC 2013 Conference, http://accelconf.web.cern.ch/AccelConf/IPAC2013/papers/tupea004.pdf.

[3] Phys. Rev. B 79, 212406 (2009).

[4] G. Moore, Opt. Commun. 52(1984)46.

[5] E.L. Saldin, E.A. Schneidmiller, and M.V. Yurkov, Opt. Commun. 281(2008)1179.

[6] E.L. Saldin, E.A. Schneidmiller, and M.V. Yurkov, New J. Phys. 12 (2010) 035010, doi: 10.1088/1367-2630/12/3/035010.

[7] E.L. Saldin, E.A. Schneidmiller, and M.V. Yurkov, Opt. Commun. 186(2000)185.

[8] E.L. Saldin, E.A. Schneidmiller, and M.V. Yurkov, Opt. Commun. 281(2008)4727.

[9] E.A. Schneidmiller, and M.V. Yurkov, Proc. FEL 2012 Conference, http://accelconf.web.cern.ch/AccelConf/FEL2012/papers/mopd08.pdf.

[10] E.L. Saldin, E.A. Schneidmiller, M.V. Yurkov, "The Physics of Free Electron Lasers" (Springer-Verlag, Berlin, 1999).

[11] E.L. Saldin, E.A. Schneidmiller, and M.V. Yurkov, Nucl. Instrum. and Methods A 528(2004)355.

[12] A.P. Mancuso et al., Phys. Rev. Lett. 102, 035502 (2009).

[13] A. Singer et al, Optics Express, Vol. 20, Issue 16, pp. 17480-17495 (2012)

[14] E.L. Saldin, E.A. Schneidmiller, and M.V. Yurkov, Nucl. Instrum. and Methods A 429(1999)233.

[15] M. Schmitt and C. Elliot, Phys. Rev. A, 34(1986)6.

[16] R. Bonifacio, L. De Salvo, and P. Pierini, Nucl. Instr. Meth. A 293(1990)627.

[17] W.M. Fawley, Proc. IEEE Part. Acc. Conf., 1995, p.219.

[18] H. Freund, S. Biedron and S. Milton, Nucl. Instr. Meth. A 445(2000)53.

[19] H. Freund, S. Biedron and S. Milton, IEEE J. Quant. Electr. 36(2000)275.

[20] S. Biedron et al., Nucl. Instr. Meth. A 483(2002)94.

[21] S. Biedron et al., Phys. Rev. ST 5(2002)030701.

[22] Z. Huang and K. Kim, Phys. Rev. E, 62(2000)7295.

[23] Z. Huang and K. Kim, Nucl. Instr. Meth. A 475(2001)112.

[24] E.L. Saldin, E.A. Schneidmiller and M.V. Yurkov, Phys. Rev. ST-AB 9(2006)030702

[25] R. Bonifacio, C. Pellegrini and L.M. Narducci, Opt. Commun. 50(1984)373.